

01 Feb 2022

Efficient and Accurate Phase-Measurement Method for Core-Loss Characterization

Anfeng Huang

Jun Fan

Missouri University of Science and Technology, jfan@mst.edu

Chulsoon Hwang

Missouri University of Science and Technology, hwangc@mst.edu

Follow this and additional works at: https://scholarsmine.mst.edu/ele_comeng_facwork



Part of the [Electrical and Computer Engineering Commons](#)

Recommended Citation

A. Huang et al., "Efficient and Accurate Phase-Measurement Method for Core-Loss Characterization," *Review of Scientific Instruments*, vol. 93, no. 2, article no. 024701, American Institute of Physics, Feb 2022.

The definitive version is available at <https://doi.org/10.1063/5.0074290>

This Article - Journal is brought to you for free and open access by Scholars' Mine. It has been accepted for inclusion in Electrical and Computer Engineering Faculty Research & Creative Works by an authorized administrator of Scholars' Mine. This work is protected by U. S. Copyright Law. Unauthorized use including reproduction for redistribution requires the permission of the copyright holder. For more information, please contact scholarsmine@mst.edu.

Efficient and accurate phase-measurement method for core-loss characterization

Cite as: Rev. Sci. Instrum. **93**, 024701 (2022); <https://doi.org/10.1063/5.0074290>

Submitted: 07 October 2021 • Accepted: 08 January 2022 • Published Online: 01 February 2022

 Anfeng Huang,  Jun Fan and Chulsoon Hwang



View Online



Export Citation



CrossMark

ARTICLES YOU MAY BE INTERESTED IN

[Diagnostics of RF coupling in H⁻ ion sources as a tool for optimizing source design and operational parameters](#)



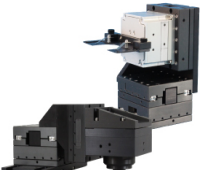
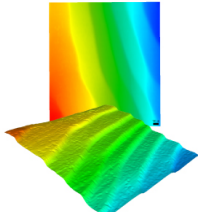
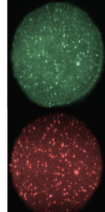
Review of Scientific Instruments **93**, 023501 (2022); <https://doi.org/10.1063/5.0077934>

[Powerful nanographite fault current limiter for smart grid](#)

Review of Scientific Instruments **93**, 024702 (2022); <https://doi.org/10.1063/5.0072005>

[Rotary table wobble error analysis and correction of a rotating accelerometer gravity gradiometer](#)

Review of Scientific Instruments **93**, 024501 (2022); <https://doi.org/10.1063/5.0077151>

 MCL MAD CITY LABS INC. www.madcitylabs.com	<p>Nanopositioning Systems</p> 	<p>Modular Motion Control</p> 	<p>AFM and NSOM Instruments</p> 	<p>Single Molecule Microscopes</p> 
---	--	--	---	--

Efficient and accurate phase-measurement method for core-loss characterization

Cite as: Rev. Sci. Instrum. 93, 024701 (2022); doi: 10.1063/5.0074290

Submitted: 7 October 2021 • Accepted: 8 January 2022 •

Published Online: 1 February 2022



Anfeng Huang,  Jun Fan,  and Chulsoon Hwang^{a)}

AFFILIATIONS

EMC Laboratory, Missouri University of Science and Technology, Rolla, Missouri 65401, USA

^{a)} Author to whom correspondence should be addressed: hwangc@mst.edu

ABSTRACT

Accurate core-loss characterization is essential to push the power density of power converters to their limits. However, existing core-loss measurement methods still have some limitations, such as a slow test speed and a complex probe calibration procedure. In particular, accurate phase-difference measurement is time-consuming because a fast Fourier transform analysis with a kHz-range frequency interval is typically applied to reduce the influence of noise. An automated measurement system for magnetic core-loss characterization is described in this paper. An accurate phase-detection block with programmable attenuators is developed to measure the phase difference between voltage and current waveforms. The proposed system considerably improves the test speed while providing comparable accuracy to the existing method.

Published under an exclusive license by AIP Publishing. <https://doi.org/10.1063/5.0074290>

The implementation of high-frequency and high-power-density switching converters is hindered by losses in magnetic components, in particular magnetic cores.¹ Several attempts have been made to establish a repeatable and accurate core-loss method under different excitations. However, none of these methods has been recognized as a reference method, and one of the main error sources is the phase error introduced by time delays of probes and oscilloscopes. The error due to phase discrepancy has been clearly presented in Ref. 2, which can be formulated as

$$\begin{aligned} P_{error} &= \tan(\theta) \cdot \Delta\theta \\ &= Q \cdot \Delta\theta, \end{aligned} \quad (1)$$

where θ represents the phase difference between the voltage and current waveforms and $\Delta\theta$ is the phase shift discrepancy between the voltage and current sensors. Q is the quality factor of the ferrite core under test (CUT). A measurement error of 100% can result from a phase error of only 0.5° .

In previous studies, a high-end oscilloscope has typically been required to accurately characterize the phase difference.³ However, these methods still suffer from the unideal characteristics of real-time oscilloscopes, e.g., port-matching and RF front-to-end error.⁴ In addition, the large analog bandwidth of an oscilloscope introduces additional noise that makes phase measurement in the time domain even more challenging. Post-analysis based on the

fast Fourier transform (FFT) is conventionally used to circumvent integrating the noise over the entire analog bandwidth but can be computationally expensive. The test speed is also a concern when a large quantity of data is expected.

In this study, an improved core-loss measurement method is implemented based on the traditional dual-winding approach. A simple and efficient, yet accurate, phase-detection block is deployed to bypass the FFT process. The test speed is 40 times higher than that of the conventional approach, demonstrating the suitability of the proposed method for massive testing. In addition, the additional phase error due to probes is eliminated by using the three-coil air-core phase shift test kit demonstrated in Ref. 5.

Figure 1 shows a block diagram of the measurement system under a sinusoidal wave excitation. A power amplifier (IFI 5500, 10 kHz–500 MHz) is used. A toroidal core under test (CUT) carries two windings with equally distributed M turns, and the current I_1 is injected into the primary winding. The magnetic induced voltage V_2 is, then, measured across the secondary side to prevent a voltage drop due to leakage inductance and resistance. The core loss P_{Core} can be calculated by measuring the time-domain waveforms of V_2 and V_1 ;³ in particular, the FFT is conventionally applied,

$$P_{Core} = \sum_{n=1}^N V_{2,N} I_{1,N} \cos(\phi_n), \quad (2)$$

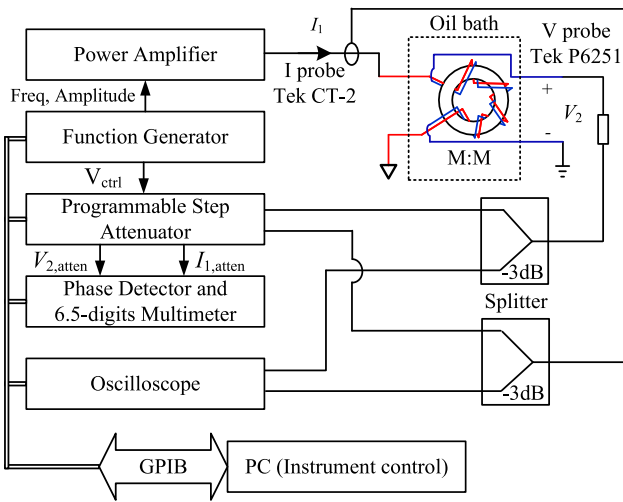


FIG. 1. The system diagram of the proposed automated measurement system.

where N is the number of harmonics and $V_{2,N}$ and $I_{1,N}$ are the amplitudes of the n -th harmonics of V_2 and I_1 , respectively. $\cos(\phi_n)$ represents the phase difference between the n -th harmonic voltage and current components.

In the proposed system, the amplitudes of both signals are measured by using an oscilloscope (Agilent MSO8104A), and the phase is measured using a phase detector that transforms the phase difference into a DC output. The circuit is designed and implemented based on the datasheet, realizing a low-frequency limit down to 1 MHz. A multimeter (Agilent 33401A) with 6.5-digit resolution is used to measure the output voltage.

Note that the accuracy of the test system is mainly determined by using the phase-detection block. The AD8302 comprises a matched pair of demodulating log amplifiers, each of which has a 60-dB measurement range. A multiplier-type phase detector is also integrated into the chip and driven by the outputs of the log amplifiers. The chip enables accurate phase measurement, independent of the signal level over a wide range. However, the phase detector has a limited input signal range (-73 to -13 dBV). Thus, a pair of programmable attenuators (HP33321H, up to 70 dB) are employed in the system to prevent saturation of the pre-amps. The amplitudes of the input signals can be controlled between -30 and -20 dBV without significantly sacrificing the signal-to-noise ratio and preventing saturation of the phase detector. In addition, two splitters (minicircuits, ZFSCJ-2-2) are used to prevent impedance mismatch between probes and instruments.

To demonstrate the phase-measurement accuracy of the test system, a signal generator is used to mimic the voltage and current signals measured in the full system, and the output sinusoidal waves are configured at 5 MHz and $0.4 V_{pk-pk}$, as shown in Fig. 2. The deviation in the phase between the two signals is swept from 75° to 95° with a step of 0.1° . The error introduced by the step attenuator is also tested for 0, 10, and 20 dB of attenuation. Note that the sensitivity of the phase detector is set at 11 mV/deg.

As illustrated in Fig. 3, the measured phase differences closely follow the set values over the entire test range and under

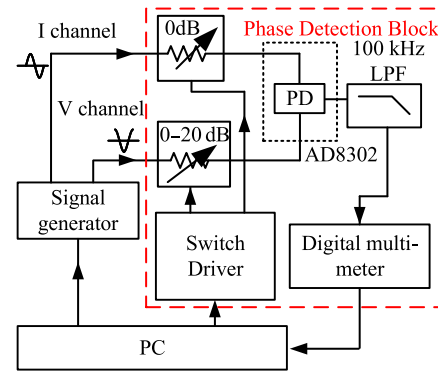


FIG. 2. Characterization setup for the phase detector and programmable attenuators.

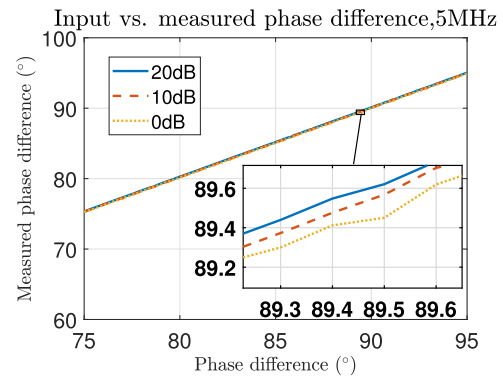


FIG. 3. Comparison between the input and measured phase deviation.

different attenuations. The plotted zoomed-in results show the additional phase shift introduced by the attenuator. This additional phase error is limited to 0.1° for 20 dB of attenuation. This error is typically negligible for most applications, and the phase shift can be calibrated out using a three-coil test kit, as will be described later.

Another experiment is performed using the histogram technique to test the noise in phase measurement, and the result is shown in Fig. 4. 100 measurements are performed when the phase differences between the two channels are set at 89° , 89.1° , and 89.2° . The result indicates that the variation in the phase shift is controlled to within 0.15° if we assume that the signal generator is ideal. Higher phase resolution can be achieved by averaging the results from multiple measurements.

Although the phase deviation between the two input channels can be accurately measured, the imbalance in phase shifts due to cables, probes, and power splitters still needs to be compensated for. A three-coil test kit is developed based on Ref. 5 to calibrate the additional phase error, and the configuration is shown in Fig. 5. The complete system contains three loosely coupled air-core coils, and the mutual impedance, which is defined as the ratio between the

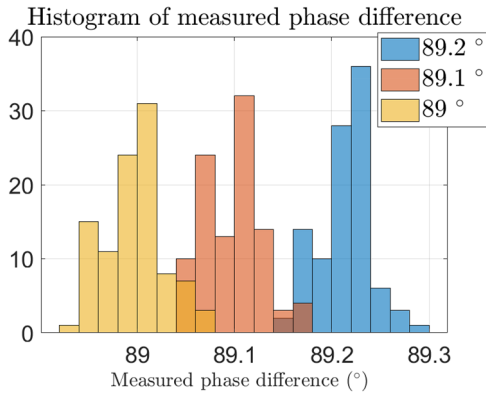


FIG. 4. Histogram of the measured phase difference. The phase differences between the input signals are swept from 89°, 89.1°, and 89.2°. The resolution of the multimeter is set to 5 $\frac{1}{2}$, and the integration time is specified as 10 PLC.

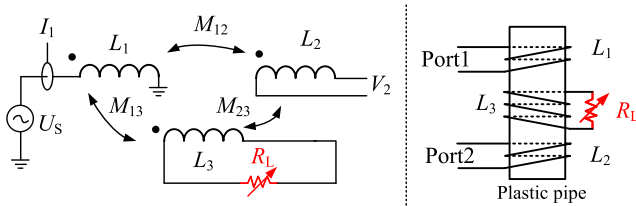


FIG. 5. Equivalent circuit of the three-coil system. L_1 , L_2 , and L_3 correspond to the self-inductance of the primary, secondary, and loading coils, respectively. M_{12} , M_{13} , and M_{23} represent the mutual inductances, and R_L is the load resistance. All three coils are fabricated by winding single-strand AWG 24 copper wires around a plastic pipe with a diameter of 6 cm.

open-circuit output voltage V_2 of coil No. 2 and the input current I_1 of coil No. 1, can be used in the probe calibration.

The air-core coils are implemented with linear components, where the mutual impedance Z_M is independent of the excitation level. Therefore, the phase of the mutual impedance Z_M can be characterized by an instrument designed for small-signal measurement, e.g., a vector network analyzer (VNA) or a gain/phase analyzer. In addition, the mutual impedance is configurable by applying different loads to coil No. 3. The mutual impedance is derived as follows:⁵

$$Z_M = \frac{V_2}{I_1} = \frac{\omega^2(M_{12}L_3 - M_{13}M_{23} - j\omega M_{12}R_L)}{R_L + j\omega L_3}, \quad (3)$$

where V_2 is the open-circuit voltage of the secondary coil and I_1 is the input current of the primary coil. Note that the mutual impedance can be directly measured by using a VNA and the phase difference Φ_{probe} between probes can be obtained by comparing the phases of Z_M measured by using the VNA and the proposed system. In the calibration process, C denotes the phase of Z_M measured by using the VNA, which serves as the reference. The phase measured

by using the proposed system is denoted as M . A superscript (n) is introduced into each label to denote the loading resistance of coil No. 3, i.e., $R_L \cdot \Phi_{probe}$ can, then, be calculated as

$$\Phi_{probe} = C^{(10 \text{ k}\Omega)} - M^{(10 \text{ k}\Omega)}. \quad (4)$$

The test case presented in this article is calibrated using a 10-k Ω load. Figure 6 compares the phases of Z_M measured by using different instruments after phase calibration. The measured phases are well-matched, which validates the proposed system. In addition, the phase error between the two methods is limited to 0.15° in the

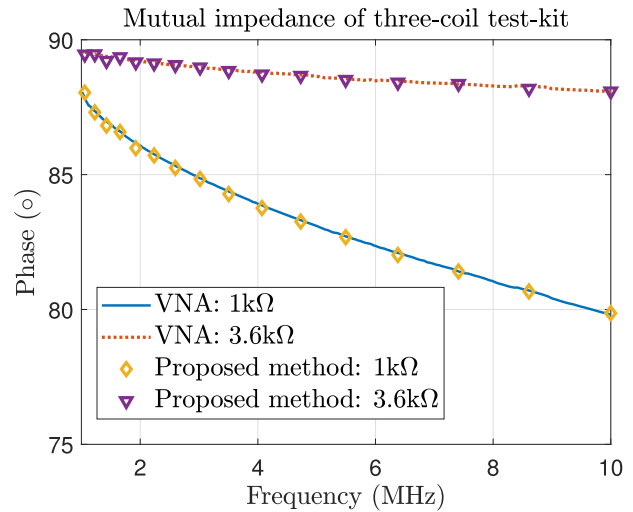


FIG. 6. Comparison of mutual impedance measured by using the VNA and scope under different loading resistances.

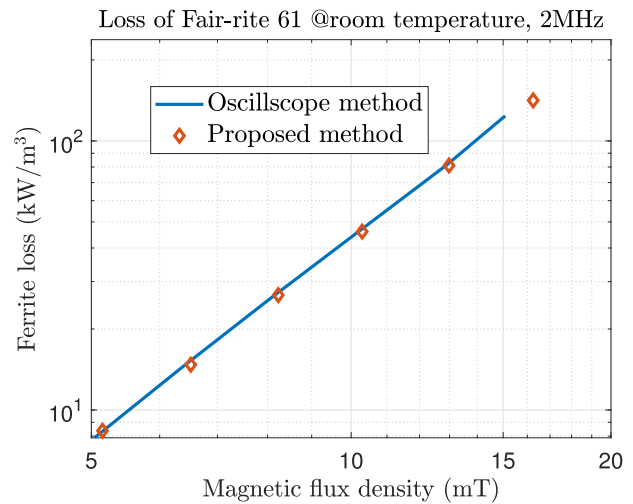


FIG. 7. Comparison between the losses measured using the conventional oscilloscope-based method and proposed method.

frequency range of 2–10 MHz. The error introduced by phase measurement is limited to 15% for a core with a quality factor under 60.² In addition to the phase error due to probes, the amplitude response of probes and power splitters should be compensated for and can also be characterized by using a VNA.

Finally, the loss of a magnetic core (Fair-rite 61, T36/23/13-61) is measured by using the proposed system and compared with that obtained using the method in Ref. 5. The CUT sample carries nine turns of uniformly distributed windings of AWG 24 copper wires. The results are shown in Fig. 7. The difference between the core losses measured by using the conventional oscilloscope-based method and the proposed method is limited to 8%. Note that the proposed method has a considerably higher test speed than the conventional oscilloscope-based method. For instance, the total measurement time for a single data point is ~40 s using the FFT-based method, including data transfer (with Agilent MSO8104A, 100 M/Sa, 500-k record length) and FFT calculation. The measurement time can be reduced to ~1 s using the proposed system, which is, therefore, suitable for applications involving massive test data. However, the proposed method is not valid in the presence of strong distortion. In addition, the resonance method is suggested for cores with ultrahigh Q.²

This study is based on research that was supported, in part, by the National Science Foundation under Grant No. IIP-1916535.

AUTHOR DECLARATIONS

Conflict of Interest

The authors have no conflicts to disclose.

DATA AVAILABILITY

The data that support the findings of this study are available from the corresponding author upon reasonable request.

REFERENCES

- ¹R. S. Yang, A. J. Hanson, B. A. Reese, C. R. Sullivan, and D. J. Perreault, “A low-loss inductor structure and design guidelines for high-frequency applications,” *IEEE Trans. Power Electron.* **34**, 9993–10005 (2019).
- ²M. Mu, Q. Li, D. J. Gilham, F. C. Lee, and K. D. Ngo, “New core loss measurement method for high-frequency magnetic materials,” *IEEE Trans. Power Electron.* **29**, 4374–4381 (2013).
- ³A. J. Batista, J. C. S. Fagundes, and P. Viarouge, “An automated measurement system for core loss characterization,” *IEEE Trans. Instrum. Meas.* **48**, 663–667 (1999).
- ⁴S. Gustafsson, M. Thorsell, J. Stenarson, and C. Fager, “An oscilloscope correction method for vector-corrected rf measurements,” *IEEE Trans. Instrum. Meas.* **64**, 2541–2547 (2015).
- ⁵A. Huang, H. Kim, H. Zhang, Q. He, D. Pommerenke, and J. Fan, “An impedance converter-based probe characterization method for magnetic materials loss measurement,” *IEEE J. Emerging Sel. Top. Power Electron.* (published online 2021).